Simulation Studies of Plasmon Enhanced Evanescent Near-Field Optical Lithography

B.Sefa-Ntiri*, P.Docker, M.C.Ward and P.D.Prewett

*Research Centre for MicroEngineering and Nanotechnology, The University of Birmingham
B15 2TT, United Kingdom
* bxs163@bham.ac.uk

ABSTRACT

A finite element analysis (FEA) of surface plasmon polariton (SPP) assisted evanescent near field optical lithography (ENFOL) is described. A gold on silicon nitride nanostructured, low-stress, conformable mask is used to control the coupling between surface plasmons (SPs) and the incident light, in conjunction with an optically active resist, to couple the SPs and the transmitted evanescent field for in lithography.

Keywords: surface plasmons photonics, evanescent field

1 INTRODUCTION

Photonic technology, coupled with nanotechnology meet many of the present day revolutionary challenges in communications, computer memory, and data processing [1]. Because of this, there is currently great interest in the optical properties of micro-/nanostructures [2]. One of the principal reasons for the upsurge of interest in this field is that micro-/nanostructures such as apertures (slits) smaller than the wavelength of light can lead to localization of electromagnetic fields, overcoming the diffraction limit of conventional optics [3]. This has great potential for novel optical devices and may also be used to extend the range of optical lithography into the nanoscale.

Among the best candidates to act as the elementary components of such devices are nanoscale structures of noble metals [4]. These materials are able to sustain resonant electron oscillations (plasmons) in the electron gas. Surface plasmons give rise to a spectrally selective optical response and a local field enhancement of the radiation which can be used in the context of nano-optics, particularly in near-field optical lithography [5]. Several studies have given evidence for extraordinarily high light transmission and of the existence of photonic energy band gaps [6,7]. These effects have been connected with surface plasmon polaritons (SPPs). However, the precise nature of the SP interaction with sub-wavelength sized structures is not yet fully understood.

Plasmon vibrations are restricted to a region of skin depth close to the interface, as seen in the expression;

$$v = \sqrt{\omega / k_x}, \qquad (1)$$

where, v, is the phase velocity of the generated propagating SPPs at the interface of the metal/dielectric. At large k_x, the value of the skin depth at which the field falls to 1/e, is given by $1/k_x$ leading to a strong concentration of the field near the interface of the metal/dielectric. According to the theory of surface plasmon optics, this value is smaller than that of the illuminating wave. The plasmons cannot be radiative since the amplitude of the field rapidly decreases perpendicularly from the metal/dielectric interface [8].

Techniques such as evanescent near-field optical lithography (ENFOL) are becoming particularly attractive with the need for the miniaturization of devices in the IC industry [9]. However, there are certain limitations which work against ENFOL as a method providing challenges for fundamental research and opportunities for nanolithography.

This paper details the work developed by us, to produce a predictive model that can be used by future workers wishing to use ENFOL. We report the recent progress achieved using FEMLAB^{TM} (version 2.3b). [FEMLAB is a registered trademark of COMSOL AB.] Our simulation studies investigate the near-field of nanometre gold 2D gratings in a low-stress Si_3N_4 membrane substrate, when normally incident p-polarized UV (λ=248nm) light is used. The model provides a tool for developing prototype low-cost, flexible and high-performance optical lithographic masks for the fabrication of high resolution features, in a "virtual testing" capability. FEMLAB is an excellent tool for an adequate description of the interaction of light and matter. Hence it is able to resolve some of the major issues affecting optical near-field lithography. With this, we have acquired a better understanding of these issues and how to overcome them. For example, we have observed a phenomenal depth of field, which hitherto was one of the major drawbacks with a stand-alone ENFOL technique. Attainment of high contrast in the image plane is demonstrated. Optical field enhancement, edge enhancement and resolution enhancement are all studied.

A metal nanostructured conformable mask is used to control the coupling between surface plasmons and the incident light and, in conjunction with an optically active resist, to couple the surface plasmons and the transmitted evanescent field, for replication of the mask features. Wit this we have developed new knowledge which provides us with the ability to design metallic nanostructured masks for the ENFOL technique.

2 THE SIMULATION MODEL

The basic principle of generating surface plasmons in this work is based on the idea that with the aid of a periodic corrugation or a prism, illumination light can couple with surface plasmon (SP) to obtain a new state named SPP, which has higher field intensity and a much shorter wavelength than that of the illumination light [9].

We have obtained a finite element analysis (FEA) of embedded nanostructured transmission gold metal absorber masks of thicknesses ranging from 45-52nm. The absorbers are embedded in the transparent background of a Si_3N_4 membrane. The model geometry is as shown schematically in Fig.1 for the simplest case. The system is the one that uses the concept of amplitude contrast between the transparent membrane and the opaque metal absorbers of the mask. We used a low-stress silicon nitride membrane of a relative permittivity $\varepsilon_r(isotropic) = 2.25$. The membrane substrate fills the gaps between the metal strips. In the region below the mask is a dielectric medium (photoresist) characterized by an ε_r (isotropic) = 2.5, (see Fig.1b).

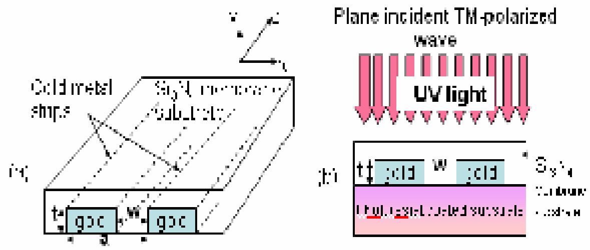

Fig.1. Metal Embedded Mask: (a) Gold metal strips of thickness, t make transmission grating mask of period a. The slit width of the grating is 30nm. (b) The geometry of the model for the simulation studies

From Fig.1, the grating mask is seen to be in conformable contact with the photoresist coated surface. Light transmits into the photoresist through the conformable mask via the slits, mediated by SPPs. The SPPs are coupled to photons by the transmitted evanescent field. We investigate the interaction of surface plasmons with individual nano-sized slits in the near-field when an in-plane TM wave (p-polarized UV, λ =248nm) illuminates a photomask at normal incidence.

When a periodically structured metal film is illuminated even at normal incidence a surface plasmon polariton can be excited on either surface of the film. A surface plasmon propagating over a grating has its dispersion relation modified from that for a flat surface. In that case, for a structured mask with deep corrugation, the resonant condition of light leaving the mask in contact with a photoresist substrate varies with parameters such as the thickness and the line width of the metal absorbers, the index of refraction of the photoresist and other details of the implementation. We consider a situation where we have no variation in the z-direction, and the magnetic field has only a z component.

The magnetic field propagates in the x-y plane. Thus, the fields can be written as [12];

$$\left.\begin{aligned} H(x,y,t) &= H_\Lambda(x,y)u_z e^{jwt} \\ E(x,y,t) &= (E_\Lambda(x,y)u_x + E_\Lambda(x,y)u_y)e^{jwt} \end{aligned}\right\} \quad (2)$$

where, u_x, u_y, u_z are unit vectors. Here we use the time-harmonic modelling (FEMLAB model H) by specifying the angular frequency. The simulation domains were either terminated with low-reflecting or perfect electric conductor/continuity boundary conditions.

3 SIMULATION RESULTS

3.1 Electric field excitation

In Fig.2, we show the finite element simulation of SP mediated ENFOL of our model. The simulated electric field of the SPPs propagating on the metal/dielectric interfaces on both sides of the mask is very evident. The localized lateral electric field distributions are generated by the excited SPs by either coupling with the incident wave/reflected wave, or the transmitted/ evanescent diffracted wave. Thus a surface plasmon at the incident surface resonantly drives another excitation at the transmitted interface. (This mechanism is explained in the next section). The coupling generates localized charge maxima at the interface, in particular, at the corners of the metal strips, which is a significant feature.

This results in a localized electric field in the near field regime on both sides of the metal. The strong field enhancement on both sides of the metal structures is also an indication of the excitation of surface plasmons. The amplitude of the surface electric field on the transmission side can reach much greater amplitude, depending on the thickness of the metal gratings; yet, our observation is that depending on the "phase solution", a time comes when the amplitude of the transmitted electric field is much greater than that at the illumination side. Since the illumination of the resist is mediated by SPPs, the size of the exposed area and the intensity below the mask should depend on the duration of the exposure. The field strength is highest on the top and bottom part of the slit, particularly, within a few nanometres perpendicularly.

A standing wave forms inside the slit as is explained in the next section. From Fig.2, the spatial pattern of the electric field is somewhat complex at the interfaces. This pattern looks similar to all the excitation obtained with wavelengths 197 – 650nm. The explanation of this may be due to the fact that, in the near field, many in-plane Fourier components $k_{\text{in-plane}} = \pm 2\pi/a, \pm 4\pi/a, \ldots\ldots.$, where, a is the grating period. These components contribute to the coherent interference of multiple scattered SP waves [13] along the surfaces, giving rise to observable interference patterns between neighbouring slits.

This complex pattern seems to be mainly determined by the lateral divergences of the propagating SPs [14]. For these reasons, in order to replicate patterns with enhanced resolution, with the density and width of the resist pattern being the same as that of the mask features, the photoresist coated substrate must be in conformable contact with the photomask, despite the highly directional intensity range of SPPs. This should be a process demand for SPPs assisted nanolithography.

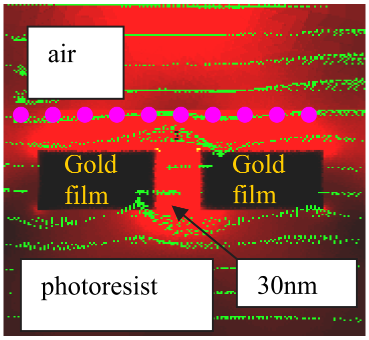

Fig.2 (colour): The simulated electric field of SPPs assisted ENFOL, using a normally incident in-plane TM wave ($\lambda = 248nm$). The arrows indicate the field mode of the excitation. The pink dots indicate the upper boundary of the membrane substrate

From Fig.3, high electric field intensity collects at the edges of the slit, particularly at the metal corners, the so called, “hot spots”. Field intensity is extreme due to surface charge localization, due to the continuity of the displacement field D = ε_mE [15]. This however, does not distort the resolution, and the feature size of the image taken at the exit plane for conformable contact optical lithography. It may, however, lead to a broader electric field distribution beyond the exit plane. If a non-contact technique is employed the distortion will affect the resolution. For this reason, we obtained time-average squared electric field intensity profiles at a few nanometre depths below the mask (see Fig.4). The intensity peaks at the edges suggest that a strong field enhancement is exhibited at the edges of the metal gratings. In fact, the same charges that provide the lateral electric field also generate a significant normal field which broadens the intensity distribution in the image plane far below the mask. This normal field distribution is an unavoidable by-product of the charge distribution required to achieve near-field imaging with planar metal films [16]. Thus, these results imply that in applications involving the use of near-field intensity, such as near-field lithography, the maximum resolution enhancement is always less than is possible for the lateral field components. However, with SPPs mediated lithography, resolution enhancement can be achieved for intimate contact photolithography.

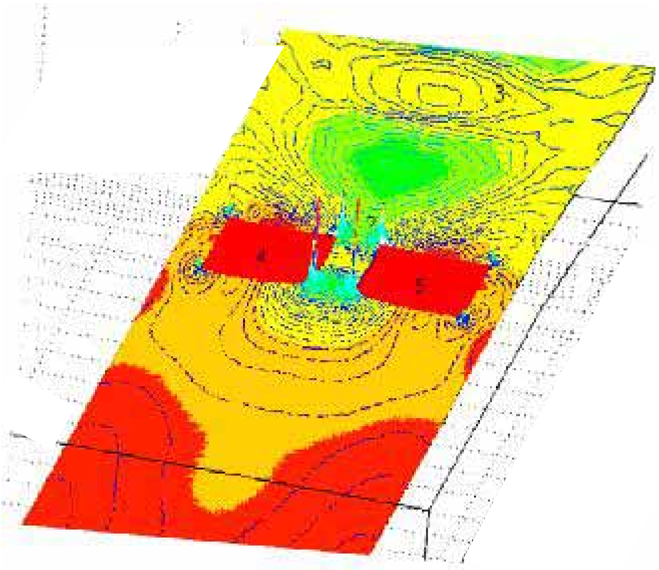

Fig.3; (colour and contour) A 3D surface plot of the simulated electric field.

3.2 Light and electromagnetic energy coupling

The incident plane wave interacts with the periodic structure of the grating, resulting in diffracted waves; reflection, and transmission with evolution of evanescent diffracted waves. The incident TM wave excites surface plasmon polariton (SPP) waves at the top and lower interfaces of the mask via the diffracted waves above and below the grating mask. This causes a surface wave to resonate between the upper and the lower ends of the slits. At the top surface of the metal/membrane interface, a photon flux $S_{x,norm}$ is transferred along the x-direction across the interface towards neighbouring slits. Thus electromagnetic energy is mainly focused into the slit, as can be seen in fig.5.

The SPP waves couple into the nanoslit, giving rise to an increase in electric energy density, $W_{eavx,norm}$ at the upper end of the slit, in addition to the input-pulse energy - a contribution from the incident plane wave which is incident normally on the upper part of the slit. The photon flux $S_{x,norm}$ on the upper surface continues to flow. This is due to the lifetime of the surface plasmon excitations, which may be longer than the input wave duration. The increase in energy at the top part of the slit drives a photon flux $S_{y,norm}$ In contrast, the energy level of the $W_{eavx,norm}$ on the lower interface of the set-up is high at this moment when that at the top has disappeared.

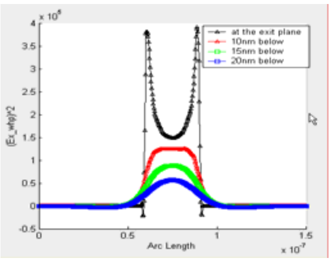

Fig.4: Time average square electric field intensity profiles at varying depths below the mask.

directed towards the lower end of the slit channel. Hence the energy is transferred from the upper end to the lower end of the slit. As a consequence, there is a coupling between the evanescent diffracted waves and the surface plasmons. The energy density inside the slit at the lower end then induces a photon flux $S_{x,norm}$ on the lower surface along x, directed away from the slit. As a result of this, the energy density $W_{eavx,norm}$ inside the slit on the upper surface begins to reduce towards zero, and, simultaneously, both the photon fluxes $S_{y,norm}$ and $S_{x,norm}$ disappear. Therefore, $W_{eavx,norm}$ is able to drive a photon flux $S_{y,norm}$ up the slit, which transfers energy from the bottom to the top surface - the reverse situation of that described before. Thus a periodic oscillation of the energy between upper and lower interfaces is induced; creating a standing wave. This oscillation is damped by scattering, absorption and Ohmic losses in the slit walls. The above scenario is graphed in Fig.5 above.

In Fig.6, we plot the time average square values of the electric field intensity, $(E_x)^2$ and $(E_y)^2$ respectively. The plots are indication of the coupling stages of SPPs at the interfaces, and through the slit. The blue line is $(E_x)^2$ along the inner left wall of the slit. The red is $(E_y)^2$ along the same path as $(E_x)^2$. The black line is through the centre of the slit.

The magnitudes of the intensities change in terms of the phase solutions.

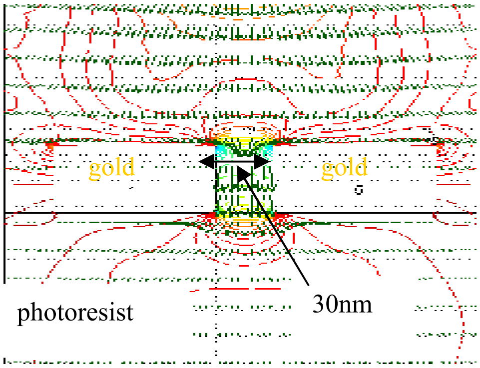

Fig 5: Average power flow.

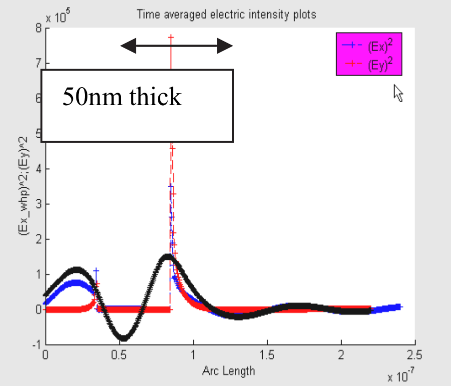

Fig.6; Time average square electric field intensity plots from top to the bottom surfaces.

4 CONCLUSIONS

We have used a finite element method to provide a critical assessment of the viability of surface plasmons for nanolithography and the potential of ENFOL as a variant of contact photolithography has been ascertained. In view of the rapidly growing importance of nanoscale devices, the microscopic understanding of the physical processes involved in the interaction of light and matter has considerable practical relevance for nanolithography.

REFERENCES

[1] Paras N. Prasad, “Nanophotonics,” Wiley Interscience, USA, 2004

[2] S.C. Kitson, W.L. Barnes and J.R. Samble, Phys. Rev. Lett. 77, 2670, 1996.

[3] M.M.J. Treacy, Appl. Phys. Lett. 75, 606, 1999.

[4] J.R. Krenn *et al.*, J. of Microscopy, 202, 122, 2001.

[5] J.J. Kuta et *al*., J. Opt. Soc. Am. A12, 1118, 1995.

[6] T.W. Ebbessen *et al*., Nature (London), 391, 687, 1998.

[7] W.L. Barnes *et al*., Phys. Rev. B 54, 6227, 1996.

[8] H. Raether, Surface Plasmons, Springer Tracts in Modern Physics 111.Springer-Verlag, Berlin, 1988.

[9] S.J. McNab, R.J. Blaikie and M.M. Alkaisi, J. Vac. Sci. Technol. B 18(6), 2900, 2000.

[10] H. Raether, “Surface Plasmons on Smooth and Rough Surfaces and on Gratings,” Springer, Heidelberg, 1988.

[11] L. Salomon *et al*., Phys. Rev. Letts. 86, 1110, 2001.

[12] Femlab (version 2.3) Reference Manual.

[13] Xiangang Luo and Teruga Ishihara, Appl. Phys. Letts. 84, 4780, 2004.

[14] R.D. Grober, T. Rutherford and T.D. Harris, Appl. Opt. 35, 3488, 1996.

[15] Micheal Paulus *et al.*, Microelectronic Engineering, 57-58, 109, 2001.

[16] S.I. Bozhevolnyi *et al*., Opt. Lett. 26, 734, 2001.